

The Physical Interpretation of Optical Spectra of High Redshift Galaxies

Henry J. Pearce*

1 Introduction

In observational astronomy the most basic observation that can be made is how bright an astronomical object is in a single wavelength band i.e. its apparent magnitude. More details of an object can be acquired by making photometric observations in different bands e.g. colours and estimates of redshift, mass and age. The next step towards gathering data about an astronomical object is to take a spectrum of the object. This can be done over a variety of wavelength ranges, typically optical and near infrared. A lot more details can be retrieved from spectra as opposed to photometry, for example more accurate redshifts estimations, metallicity and dynamical measurements. Spectroscopy involves the dispersion of the light from the entire scale length of an astronomical object or region but further information can be gathered by performing integral field spectroscopy. Using an integral field unit (IFU) you can disperse the light of every pixel in the field of view.

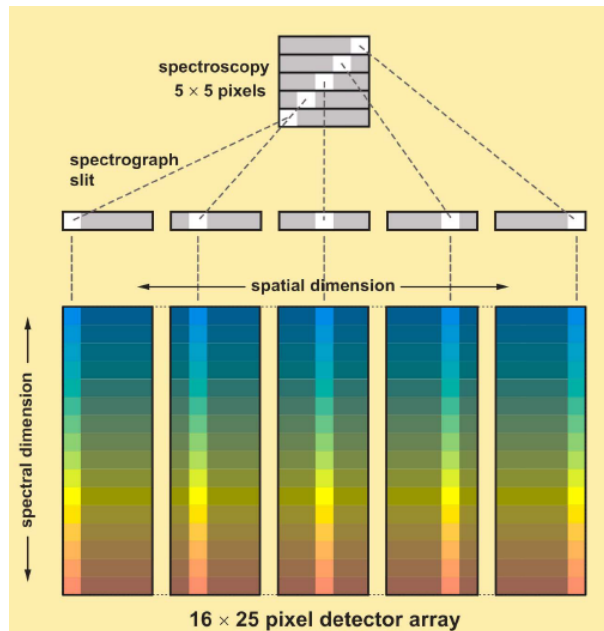


Figure 1: Integral field spectroscopy

*hjp@roe.ac.uk

Spectral features (emission and absorption) originate from the interaction between the photons produced by the stellar population and the surrounding neutral hydrogen. The emitted photons ionize the neutral gas, resulting in absorption features, and then when the gas recombines a photon is re-emitted, resulting in emission features. From spectra you can easily see that galaxies evolve with age. Young late-type galaxies have a blue spectrum with emission lines. As they age their spectra becomes redder as the stellar populations age and the galaxy increases in metallicity increasing the number and strength of absorption features.

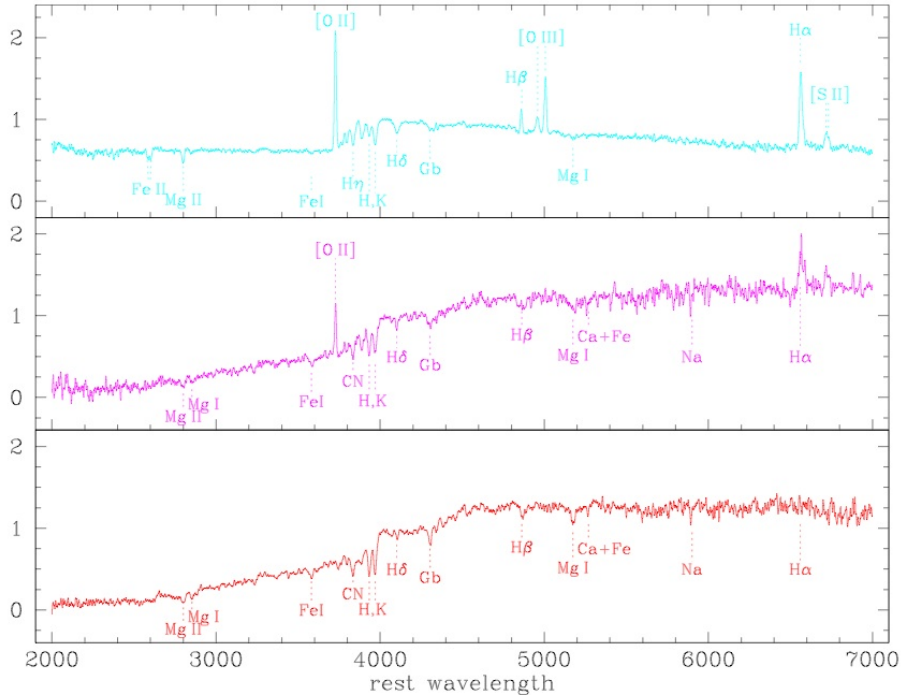


Figure 2: The composite spectra from the K20 sample Mignoli et al. (2005). The cyan, purple and red spectra correspond to emission line, intermediate and early-type galaxies respectively.

But galaxy identification is not as simple as this as there is an age/metallicity degeneracy since more metals implies more opacity and absorption in the blue wavelengths which leads to redder colours (Worthey (1994)). So an old metal-poor galaxy can have a similar spectrum to a young metal-rich galaxy. So more details are needed to determine the state of evolution of the galaxy, this will be discussed below.

2 Redshift

One of the most fundamental reasons for obtaining a spectrum of an object is to pin down more accurately the redshift. A spectral redshift is more accurate than a photometric one. A redshift can be estimated through several methods:

Spectral features - Identify spectral features (emission and/or absorption lines) and compare their wavelength to the laboratory measurements. The redshift can then be

simply calculated with the following relation,

$$z = \frac{\lambda_{obs} - \lambda_{emit}}{\lambda_{emit}} \quad (1)$$

The more features matching one redshift the more robust the estimation is. Some common features used for redshift determination for the high- z universe in optical spectra are Lyman series, Balmer series, MgI 2852.2, MgII 2796.4,2799,2803.5 (often blended), OII 3726.2,3728.9(often blended), OIII 4959,5007, CaII H & K 3933.7 3968.5.

Template fitting - Here take a variety of good signal-to-noise templates of galaxy spectra of different types (ranging from emission line galaxies, late types to passive galaxies, early types), normalise them to your spectrum and while shifting the template along in wavelength (i.e redshift) calculate the reduced χ^2 ,

$$\chi^2(z) = \sum_i \left(\frac{F_{obs,i} - bF_{model,i}}{\sigma_i^2} \right), \quad (2)$$

where F_{obs} = the observed flux, F_{model} = the corresponding value of your template, b = normalisation factor and σ = the error, between your spectrum and the template. The template and redshift with the minimum χ^2 gives you your best redshift estimate. Therefore also from template fitting you also can acquire an idea of the type of galaxy your target is.

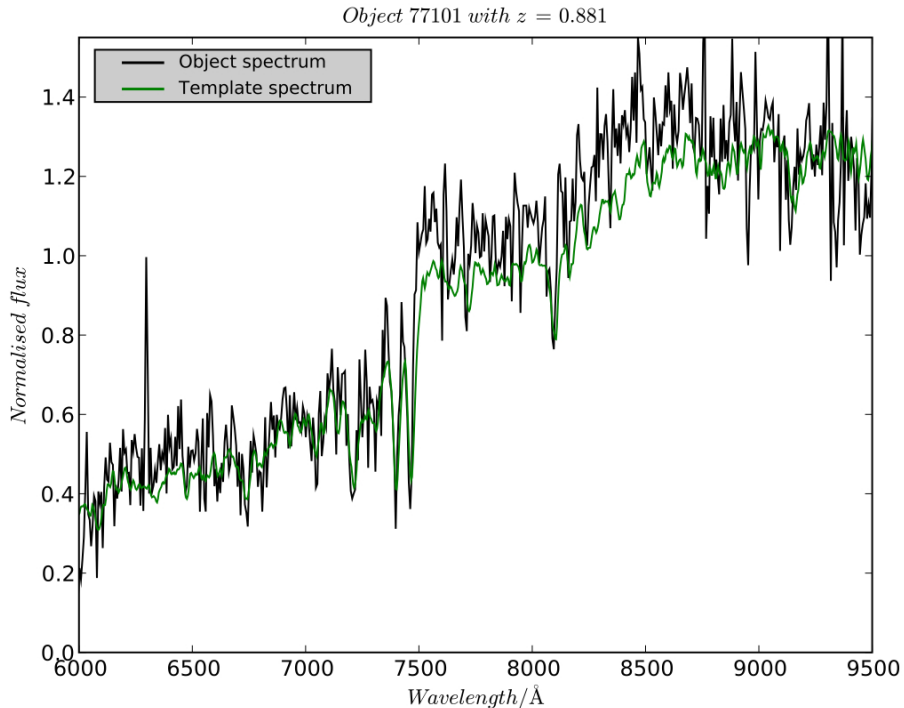


Figure 3: Example of galaxy with good fit to an early-type template

Cross correlation - As for template fitting take a set of good signal-to-noise galaxy templates normalised to your target spectrum and shift the template along in wavelength (i.e. redshift) calculating the integral of their product after each shift. But as

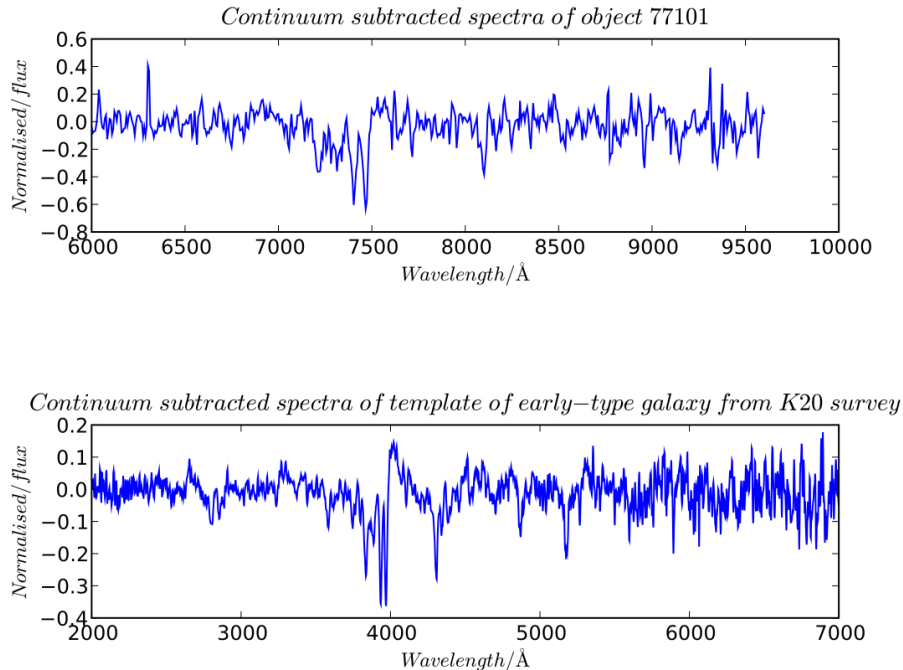


Figure 4: Example of galaxy and template with continuum subtracted spectra to be used for cross correlation

your spectrum is a discrete function you should use the following function,

$$(f \star g)(n) = \sum_{m=-\infty}^{\infty} f(m)g(n+m) \quad (3)$$

The best match for template and redshift is the maximum of this function. But since estimations of redshifts are often acquired by matching features so it can sometimes be beneficial to continuum subtract your spectra and the template before performing the cross correlation. This will give the best fit to the one that matches the most spectral features. Even though through removing the continuum you have lost any shape information from the fit but it will still give you an reasonable idea of the type of galaxy that gave the best fit.

3 Dynamics

3.1 Velocity Dispersion

Velocity dispersion is the variance of the velocity distribution of the stellar population within a galactic system. One method for determining the velocity dispersion in high redshift galaxies is via stellar absorption lines. The assumption is that the stellar absorption lines you see in high- z galactic spectra are a convolution of the absorption feature you would see in a single star and broadening function that will correspond to the velocity distribution along the line of sight. The line profiles of the absorption features are usually assumed to be Gaussian, this is because the shape

of the spectral features is the convolution of the atomic spectral feature and the instrumental broadening function. Common absorption features in optical spectra of the high- z universe are CaII H & K lines. This absorption feature is a dominant

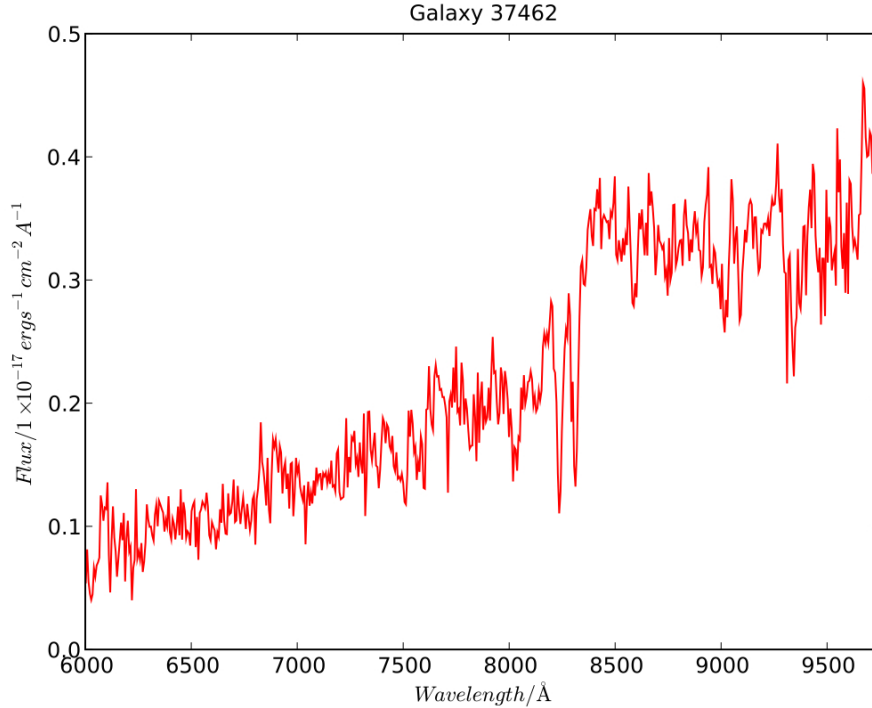


Figure 5: Example of galaxy spectra with strong CaII H & K absorption features

feature in stellar types F through to K.

To calculate the velocity dispersion take the spectrum of your galaxy and various stellar templates of F - K type stars and continuum subtract them. Convolve the continuum subtracted stellar templates with a selection of Gaussians, with different widths, as to resemble different broadenings. Then cross correlate, as mentioned earlier, to find the convolved stellar template that best matches you spectra. This would usually be done after you have the redshift for the galaxy so can deredshift the galaxy and then only perform one cross correlation calculation per template as opposed to shifting the template.

If you look at what we have just done mathematically is it easy to derive an estimate for the velocity dispersion of your galaxy. Here I will assume we are working with a single spectral feature (e.g. CaII H). Assume you have performed the cross correlation and you have the best template that matches your galaxy. Assume the stellar absorption feature can be fit with a Gaussian,

$$f_*(\lambda) = \frac{1}{\sigma_*\sqrt{2\pi}} e^{-\frac{(\lambda-\mu_*)^2}{2\sigma_*^2}}, \quad f_{bf}(\lambda) = \frac{1}{\sigma_{bf}\sqrt{2\pi}} e^{-\frac{(\lambda-\mu_{bf})^2}{2\sigma_{bf}^2}}, \quad (4)$$

where f_* and f_{bf} is the Gaussian describing the stellar absorption feature broadening function respectively. Using the convolution theorem,

$$\mathfrak{F}(f(x) \star g(x)) = \mathfrak{F}(f)\mathfrak{G}(g), \quad (5)$$

Main Sequence G0 – K5

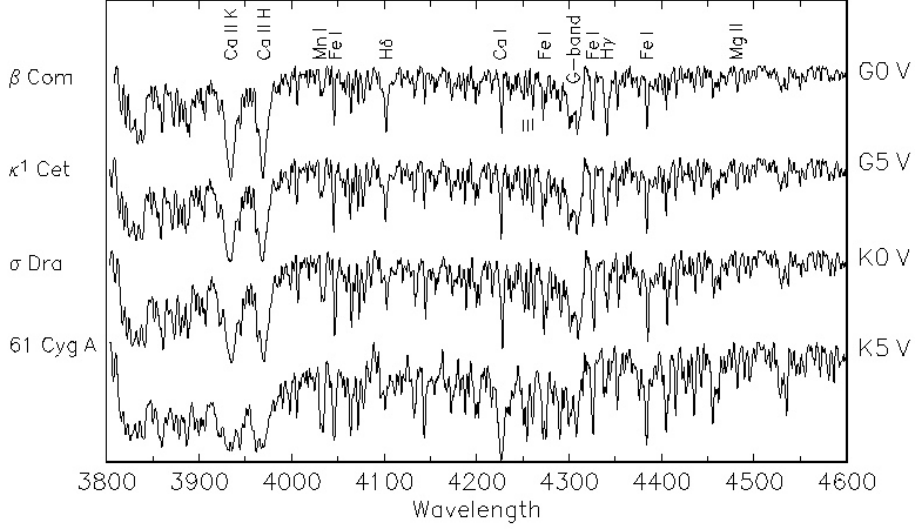


Figure 6: Spectra of various G-K type stars from A Digital Spectral Classification Atlas (Gray)

and the fact that the Fourier transform of a Gauss function is itself, the convolution the two above Gaussians is,

$$f_{best}(\lambda) = \frac{1}{(\sigma_* + \sigma_{bf})\sqrt{2\pi}} e^{-\frac{(\lambda - (\mu_* + \mu_{bf}))^2}{2(\sigma_*^2 + \sigma_{bf}^2)}}, \quad (6)$$

where f_{best} is the Gaussian function describing the best fitting to galaxy absorption feature. Therefore the σ^2 s of two convolved Gaussians add in quadrature. So once you get the best match from the cross-correlation process your velocity dispersion can be found by,

$$\sigma_{gal}^2 = \sigma_{best}^2 - \sigma_*^2, \quad (7)$$

3.2 Dynamical Mass

Once you have the velocity dispersion you can simply use the Virial Theorem to deduce an estimate for the dynamical (all mass within radius of galaxy, dark and baryonic matter) mass,

$$KE = -\frac{1}{2}PE. \quad (8)$$

This can be written as,

$$\frac{1}{2} \sum_{i \in stars} m_i \langle v^2 \rangle \simeq \frac{1}{2} \frac{GM_{dyn} \sum_{i \in stars} m_i}{R_{dyn}}. \quad (9)$$

Out to the radius of the galaxy the dominant component of matter is baryonic so we can use the approximation $\sum_{i \in stars} m_i = M_{dyn}$, which gives us,

$$\frac{1}{2} M_{dyn} \langle v^2 \rangle \simeq \frac{1}{2} \frac{GM_{dyn}^2}{R_{dyn}} \quad (10)$$

The average velocity squared can be thought of as the total velocity dispersion for the system i.e. $\langle v^2 \rangle = \sigma_{total}^2$. The total velocity distribution can be described as,

$$\sigma_{total}^2 = \sigma_x^2 + \sigma_y^2 + \sigma_z^2 \quad (11)$$

Assume the line of sight velocity dispersion we have measured is σ_x^2 . We can also assume that for a spherical system the velocity distribution in any other direction should not be any different to the one we have measured so, $\sigma_{los}^2 = \sigma_x^2 = \sigma_y^2 = \sigma_z^2$ therefore,

$$\langle v^2 \rangle = \sigma_{total}^2 = 3\sigma_{los}^2. \quad (12)$$

So the dynamical mass can be estimated as follows,

$$M_{dyn} \simeq \frac{3R_{dyn}\sigma^2}{G}. \quad (13)$$

where R_{gal} = radius of galaxy and G = universal gravitational constant.

3.3 Stellar Mass

The stellar mass can be recovered from Spectral Energy Distribution (SED) fitting. This is where photometry of your galaxy is fit with variety of synthetic stellar population templates (SSPs). If you have the spectroscopic redshift for your target then this can take away the redshift as a variable parameter in the fitting code and it will simply find the stellar population that best fits your photometry at that redshift.

The SSPs comprise of a variety of stellar populations varying in age, metallicity and

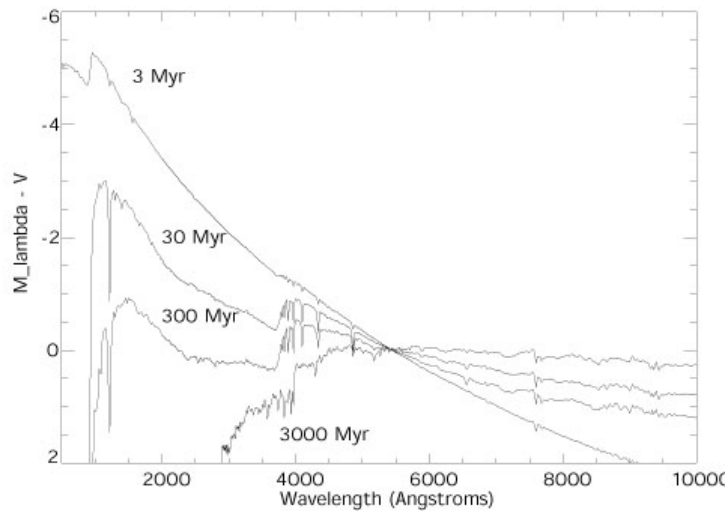


Figure 7: Example of SSPs with varying ages (Bruzual A. and Charlot (1993))

star formation history. All the SSP templates are normalised to a system with mass $1M_{\odot}$ so once you have the best fit an estimate of the stellar mass of your galaxy is the normalisation factor required to scale the template up to your photometry. Having the spectra as well can be used a check that the fitting code is doing a good job of template fitting.

4 Age & Metallicity

4.1 Stellar Metallicity

The metallicity of a galaxy can be measured through the strengths of various features and regions within the spectrum of a galaxy. The basic idea to measuring the metallicity of a galaxy is to measure the absorption or emission strength of the spectral lines of the metals. This can be done by measuring the *equivalent width* (EW) of the absorption or emission features you are interested in. The EW is defined as the area between the spectral feature and the continuum of a normalised spectrum of the object,

$$EW = \int \frac{F(\lambda) - F(c)}{F(c)} d\lambda, \quad (14)$$

where $F(c)$ is the value of the normalised continuum level and $F(\lambda)$ is the line profile function, as mentioned earlier this is often a Gaussian. The EW is the width of the unit height rectangle containing the same area as the spectral feature and can be thought of as the strength of the feature relative to the continuum. This definition gives positive values for emission lines and negative for absorption. Often the continuum

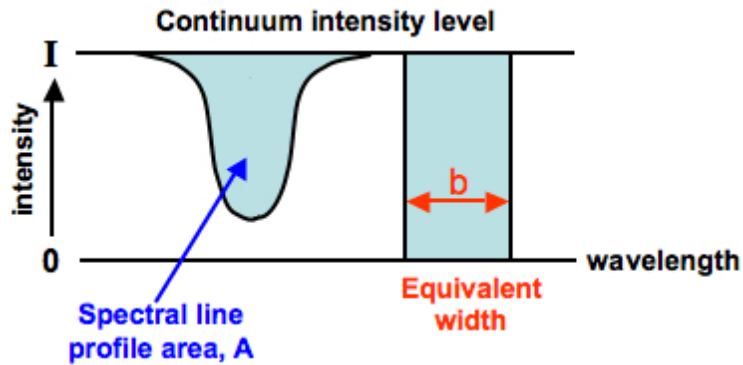


Figure 8: Diagram showing the definition of Equivalent Width

of the spectrum is noisy so $F(c)$ will have to be a continuum fit to the whole spectra or you can do a linear fit connecting the start and end of the spectral feature. Once you have your EW you must remember (unless you have deredshifted your spectrum) that you have measured a redshifted EW so you must adjust this measurement to the rest frame

$$EW_{rest} = \frac{EW_{obs}}{1+z} \quad (15)$$

In optical spectroscopy of the high- z universe you do not have access to temperature sensitive line ratios such as [SII]4070/6720, [OII]7325/3727 to empirically work out abundances. If your target is at $z \approx 1$ then you may just get the [OIII] line ratio [OIII]4363/5007. So to find calibrators for metallicity you have to look at photoionisation models. The derivation of this calibrator is a subject in itself and I will just show the results.

Note - When calculating the metallicity of a system you need to account for dust as this will, along with the hydrogen, absorb the ionising photon therefore decrease the strength of the Balmer lines and reduce the equivalent width of $H\beta$ line. But as the EW of a feature is its strength relative to stellar continuum the EW will not be effected by

dust if the emission feature region and stellar continuum experience different amounts of reddening.

I will go through a few metallicity calibrators examples that are useful for high redshift targets:

R_{23} index

The metallicity can be derived the ratio of emission line fluxes or emission line EWs. The most commonly used ratio is R_{23} , Pagel et al. (1979),

$$\log R_{23} = \log \left(\frac{EW([OII]3727) + EW([OIII]4959, 5007)}{EW(H\beta)} \right). \quad (16)$$

This is then converted to a metallicity via the relation (Zaritsky et al. (1994)),

$$12 + \log(O/H) = 9.265 - 0.33x - 0.202x^2 - 0.207x^3 - 0.33x^4, \quad (17)$$

where $x = \log(R_{23})$, and then the relation (Anders and Grevesse (1989)),

$$Z \approx 29 \times 10^{[12 + \log(O/H)] - 12} Z_{\odot}. \quad (18)$$

But as well as the metallicity the R_{23} parameter is sensitive to the ionisation state of the gas so the O_{32} paramter can be used to correct for the ionisation (Kewley and Dopita (2002), McGaugh (1991)),

$$\log O_{32} = \log \left(\frac{EW([OIII]4959, 5007)}{EW([OII]3737)} \right). \quad (19)$$

With this the corrected oxygen abundance can be derived via (Kobulnicky and Kewley (2004)),

$$\begin{aligned} 12 + \log(O/H) = & 9.11 - 0.218x - 0.0587x^2 - 0.330x^3 - 0.199x^4 - \\ & y(0.00235 - 0.1105x - 0.051x^2 - \\ & 0.04085x^3 - 0.003585x^4) \end{aligned} \quad (20)$$

1978Å index

The iron abundance stellar metallicity of a galaxy can be measured using the 1978Å index defined by Rix et al. (2004).

The studies of Thompson et al. (1974) and Swings et al. (1976) indicated that many of the absorption features between 1800 – 2200Å of star-forming galaxies are FeIII transitions. Heckman et al. (1998) showed, from a sample of ≈ 20 galaxies, that this feature of FeIII transitions becomes stronger with increasing metallicity. From the comparison of synthetic stellar spectra of different metallicity (produced by the WM-basic code) with two spectra of high- z star forming galaxies, Rix et al. (2004) went on to confirm that the strength of the FeIII feature does increase with metallicity.

rix fig

To ensure to avoid other strong features in this region they defined the *1978Å index* as the equivalent width between 1935 - 2020Å. They showed that the 1978Å index increases monotonically with metallicity. The 1978Å index measures the photospheric absorption line of FeIII of massive OB stars, the most recent stars to form in the ISM. Once you have the EW of the 1978 index it can be converted to a metallicity by,

$$\log \left(\frac{Z}{Z_{\odot}} \right) = C \times EW(1978) + D, \quad (21)$$

where

$$\begin{cases} C = 0.33 & \& D = -1.94 & EW(1978) \leq 5.9\text{\AA} \\ C = 0.42 & \& D = -2.50 & EW(1978) > 5.9\text{\AA} \end{cases}$$

4.2 Interstellar Medium Metallicity

Using features in your galaxy spectrum it is also possible to make an estimate of the metallicity of the ISM. One method for doing this is to use the *curve of growth* (Spitzer (1978)). This is a plot that shows the relationship between EW and the number of atoms per unit area producing the absorption feature i.e. a measure of the column density. A theoretical curve for this can be derived through the theory of radiative transfer. The relationship between EW and optical depth for an optical thin medium is linear, then for a moderate optical depth ($\tau > 5$) the EW scales with the log of the square root of the optical depth and when the optical depth becomes very high the EW scale with the square root of the optical depth. Then comparing your measurements of EW for the spectral features you are using a column density and therefore metallicity can be derived.

Common features to be used in high- z optical astronomy are the FeII 2374,2382 and the MgII 2796,2803 doublets.

4.3 Age

The strength of the break in the spectra of stellar systems at 4000Å, D4000, gives you an indication of the cumulative star formation history which in turn gives you an idea of the age of the system. D4000 is measured by measuring the amplitude of the break. This is done by calculating the ratio in the bands 4050-4250Å and 3750-3950Å around the 4000Å break. The understanding of how this break evolves with time is looked at using evolutionary models of galaxies (?). These models take stellar libraries, a star formation rate and an IMF and try to predict how the spectra of stellar systems will evolve. So once you have measured D4000 for your target object and have an evolutionary models that gets a good match to your spectrum you can recover an age estimate for the system.

The 4000Å break is the accumulation of ionized metal absorption lines in the atmosphere of the stars (two of the strong feature being CaII H & K). As the stellar temperature decreases the opacity of the star increase and the so does the strength of the break.

The age of a galaxy can also be estimated by fitting SSPs to the photometry of your object, as described for the stellar mass, using the spectroscopic redshift as a constraint to the model fitting.

5 Star Formation Rates

Optical spectra of the high- z galaxies contain several star formation rate (SFR) indicators. They all come from integrated light measurement in emission lines. These can be broke down into two categories:

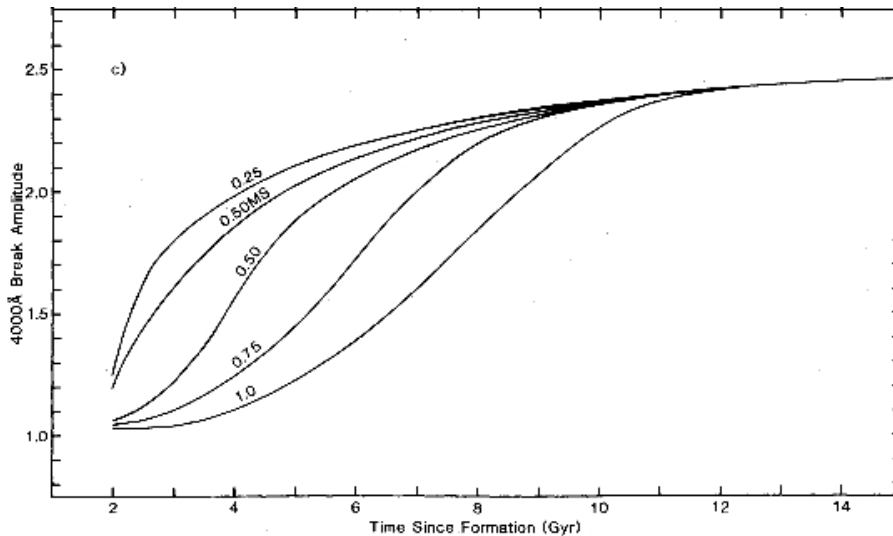


Figure 9: Plot showing predicted strength of 4000Å break against age of galaxy from evolutionary models of different e -folding times from ?

5.1 Recombination Lines

As mentioned in the introduction the light from the young massive ($M_* > 10M_\odot$) stellar population is absorbed and re-emitted by the surrounding nebula. The light from the stars ionizes the surrounding nebula and when the atoms recombine a photon of specific wavelength is released resulting in an emission line in the stellar spectrum. Since only massive stars with lifetimes $< 20 Myr$ contribute significantly to the ionizing flux these emission lines give you a direct measure of the instantaneous SFR. For an ionisation-bounded region of HII gas the Balmer emission series (lines that are emitted when the electron in an hydrogen atom makes the transition from a higher energy level to the energy level $n = 2$) directly scales with the ionising flux of the stellar population within. The most commonly used emission line is therefore the first in the Balmer series, $H\alpha$, as it is the most luminous. So the $H\alpha$ line occurs when the electron cascades down from $n = 3$ to $n = 2$ and emits a photon of wavelength 6562.8Å. Another major advantage of the $H\alpha$ line is that it is sensitive to all types of stellar population and is independent of temperature and ionisation level of the gas. Often when you measure the EW of the $H\alpha$ line you are measuring the EW of the $H\alpha + NII$ as these often can not be resolved. Several authors have published calibrations how to convert luminosity of the $H\alpha$ line in to a SFR. A commonly used one is from Kennicutt et al. (1994),

$$SFR(M_\odot \text{ year}^{-1}) = 7.9 \times 10^{-42} L(H\alpha) \text{ (ergs s}^{-1}\text{)}. \quad (22)$$

This calibration is dependent on stellar evolution and atmosphere models but is mainly limited by uncertainties in extinction and the chosen *initial mass function* (IMF). Mean extinctions have been measured (Kennicutt (1983), Niklas et al. (1997), Caplan and Deharveng (1986), Kaufman et al. (1987), van der Hulst et al. (1988), Caplan et al. (1996)) between $A(H\alpha) = 0.5 - 1.8$ mag. Since the $H\alpha$ flux is solely related to stars with $M_* > 10M_\odot$ the choice of IMF can have a massive effect on your SFRs.

Other lines in the Balmer series can be used to estimate SFRs but are much weaker as stellar absorption starts to over power the nebula emission so you are restricted to

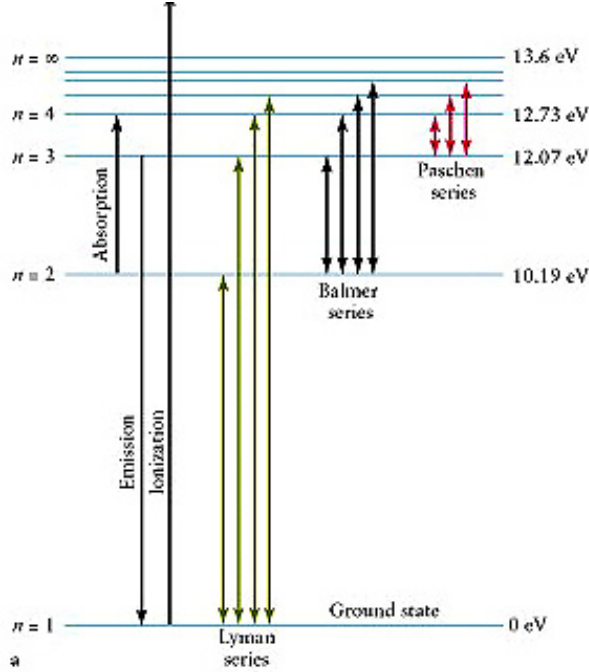


Figure 10: Diagram showing the atomic transitions of hydrogen

regions of HII with high surface brightness. This is similar for the Paschen (transitions down to energy level $n = 3$) and Brackett (transitions down to energy level $n = 4$) series.

5.2 Forbidden Lines

The $H\alpha$ line is out of the optical window after $z \approx 0.5$ so a bluer emission line is required as a SFR indicator. The next strongest emission blue-ward is the forbidden-line doublet [OII]. Being a collisionally excited line it is effected by the ionization state and the abundance of the gas and is therefore it does not trace the star formation directly. But the excitation of the [OII] line can be calibrated using $H\alpha$. Kennicutt (1992) calibration of [OII] as a star formation indicator comes from the relation of $EW(H\alpha+NII)$ and $EW([OII])$ which they found to be $EW([OII]) = 0.4EW(H\alpha + NII)$. Taking the average of Gallagher et al. (1989) and Kennicutt (1992) the star formation rate to [OII] relation comes out as,

$$SFR(M_{\odot} \text{ year}^{-1}) = (1.4 \pm 0.4) \times 10^{-41} L[OII] \text{ (ergs s}^{-1}\text{)}. \quad (23)$$

Gallagher et al. (1989) derived there calibration from comparing the flux levels of [OII] and $H\beta$, which they found has relation $f([OII]) = 3.2f(H\beta)$. Kewley and Dopita (2002) constructed a calibration to try and account for the reddening between [OII] and $H\alpha$ and came up with the conversion,

$$SFR(M_{\odot} \text{ year}^{-1}) = (6.58 \pm 1.65) \times 10^{-42} L[OII] \text{ (ergs s}^{-1}\text{)}. \quad (24)$$

A increase in the EW of the [OII] emission line can be seen as you move along the Hubble sequence for galaxies.

References

- E. Anders and N. Grevesse. Abundances of the elements - Meteoritic and solar. *GCA*, 53:197–214, Jan. 1989. doi: 10.1016/0016-7037(89)90286-X.
- G. Bruzual A. and S. Charlot. Spectral evolution of stellar populations using isochrone synthesis. *ApJ*, 405:538–553, Mar. 1993. doi: 10.1086/172385.
- J. Caplan and L. Deharveng. Extinction and reddening of H II regions in the Large Magellanic Cloud. *AAP*, 155:297–313, Feb. 1986.
- J. Caplan, T. Ye, L. Deharveng, A. J. Turtle, and R. C. Kennicutt. Extinction and reddening of HII regions in the Small Magellanic Cloud. *AAP*, 307:403–416, Mar. 1996.
- J. S. Gallagher, D. A. Hunter, and H. Bushouse. Star-formation rates and forbidden O II emission in blue galaxies. *AJ*, 97:700–707, Mar. 1989. doi: 10.1086/115015.
- R. . Gray. A Digital Spectral Classification Atlas.
- D. Hamilton. The spectral evolution of galaxies. I - an observational approach. *ApJ*, 297:371–389, Oct. 1985. doi: 10.1086/163537.
- T. M. Heckman, C. Robert, C. Leitherer, D. R. Garnett, and F. van der Rydt. The Ultraviolet Spectroscopic Properties of Local Starbursts: Implications at High Redshift. *ApJ*, 503:646–+, Aug. 1998. doi: 10.1086/306035.
- M. Kaufman, F. N. Bash, R. C. Kennicutt, Jr., and P. W. Hodge. Giant H II regions in M81. *ApJ*, 319:61–75, Aug. 1987. doi: 10.1086/165433.
- R. C. Kennicutt, Jr. The rate of star formation in normal disk galaxies. *ApJ*, 272:54–67, Sept. 1983. doi: 10.1086/161261.
- R. C. Kennicutt, Jr. The integrated spectra of nearby galaxies - General properties and emission-line spectra. *ApJ*, 388:310–327, Apr. 1992. doi: 10.1086/171154.
- R. C. Kennicutt, Jr., P. Tamblyn, and C. E. Congdon. Past and future star formation in disk galaxies. *ApJ*, 435:22–36, Nov. 1994. doi: 10.1086/174790.
- L. J. Kewley and M. A. Dopita. Using Strong Lines to Estimate Abundances in Extragalactic H II Regions and Starburst Galaxies. *ApJS*, 142:35–52, Sept. 2002. doi: 10.1086/341326.
- H. A. Kobulnicky and L. J. Kewley. Metallicities of 0.3z1.0 Galaxies in the GOODS-North Field. *ApJ*, 617:240–261, Dec. 2004. doi: 10.1086/425299.
- S. S. McGaugh. H II region abundances - Model oxygen line ratios. *ApJ*, 380:140–150, Oct. 1991. doi: 10.1086/170569.
- M. Mignoli, A. Cimatti, G. Zamorani, L. Pozzetti, E. Daddi, A. Renzini, T. Broadhurst, S. Cristiani, S. D’Odorico, A. Fontana, E. Giallongo, R. Gilmozzi, N. Menci, and P. Saracco. The K20 survey. VII. The spectroscopic catalogue: Spectral properties and evolution of the galaxy population. *AAP*, 437:883–897, July 2005. doi: 10.1051/0004-6361:20042434.
- S. Niklas, U. Klein, and R. Wielebinski. A radio continuum survey of Shapley-Ames galaxies at λ 2.8cm. II. Separation of thermal and non-thermal radio emission. *AAP*, 322:19–28, June 1997.

- B. E. J. Pagel, M. G. Edmunds, D. E. Blackwell, M. S. Chun, and G. Smith. On the composition of H II regions in southern galaxies. I - NGC 300 and 1365. *MNRAS*, 189:95–113, Oct. 1979.
- S. A. Rix, M. Pettini, C. Leitherer, F. Bresolin, R.-P. Kudritzki, and C. C. Steidel. Spectral Modeling of Star-forming Regions in the Ultraviolet: Stellar Metallicity Diagnostics for High-Redshift Galaxies. *ApJ*, 615:98–117, Nov. 2004. doi: 10.1086/424031.
- L. Spitzer. *Physical processes in the interstellar medium*. 1978.
- J. P. Swings, M. Klutz, E. Peytremann, and J. M. Vreux. Fe III lines in the ultraviolet spectra of early B stars. *AAPs*, 25:193–212, Aug. 1976.
- G. I. Thompson, C. M. Humphries, and K. Nandy. A Broad Absorption Region in the Ultraviolet Spectra of Early-Type Stars. *ApJL*, 187:L81+, Jan. 1974.
- J. M. van der Hulst, R. C. Kennicutt, P. C. Crane, and A. H. Rots. Radio properties and extinction of the H II regions in M51. *AAP*, 195:38–52, Apr. 1988.
- G. Worthey. Comprehensive stellar population models and the disentanglement of age and metallicity effects. *ApJs*, 95:107–149, Nov. 1994. doi: 10.1086/192096.
- D. Zaritsky, R. C. Kennicutt, Jr., and J. P. Huchra. H II regions and the abundance properties of spiral galaxies. *ApJ*, 420:87–109, Jan. 1994. doi: 10.1086/173544.